Study on behaviour of corroded RC beams strengthened with NSM CFRP rods – an experimental and finite e....

Conference Paper · June 2014

CITATION
1

READS
345

4 authors:

Bélal Almassri
Palestine Polytechnic University
15 PUBLICATIONS **37** CITATIONS
SEE PROFILE

Amjad Kreit
Institut National des Sciences Appliquées de ...
17 PUBLICATIONS **65** CITATIONS
SEE PROFILE

Firas Al-Mahmoud
University of Lorraine
37 PUBLICATIONS **321** CITATIONS
SEE PROFILE

Raoul Francois
Institut National des Sciences Appliquées de ...
149 PUBLICATIONS **2,857** CITATIONS
SEE PROFILE

STUDY ON BEHAVIOUR OF CORRODED RC BEAM STRENGTHENED WITH CFRP ROD, AN EXPERIMENTAL AND FINITE ELEMENT MODELLING STUDY

Belal Almassri, Amjad Kreit & Raoul Francois
Université de Toulouse
UPS, INSA, LMDC (Laboratoire Matériaux et Durabilité des Constructions)
135 avenue de Rangueil
31077 Toulouse CEDEX 04
France
almassri@etud.insa-toulouse.fr

Firas Al Mahmoud
University of Lorraine
Le Montet - Rue du Doyen Urion
CS 90137 54601 Villers Les Nancy
France
firas.al-mahmoud@univ-lorraine.fr

KEYWORDS: corrosion, repair, RC beams, NSM rods, failure mode, FEM, ABAQUS.

ABSTRACT
The near surface mounted reinforcement technique (NSM) is one of the promising techniques used nowadays to strengthen RC structures. In the NSM technique, the Carbon Fibre Reinforced Polymer (CFRP) rods are placed inside pre-cut grooves and are bonded to the concrete with epoxy adhesive. This paper investigates the effectiveness of repair technique with Near Surface Mounted (NSM) carbon fiber-reinforced polymer (CFRP) rods to restore the mechanical performance of corrosion-damaged RC beams; it also studies the failure mode of the repaired corroded RC beam according to experimental and numerical modeling results. Experimental results and numerical modeling results of finite element FE model using ABAQUS software are obtained on two beams: one corroded beam which was exposed to a natural corrosion for 25 years and one control beam with no corrosion; both beams were 3 meters long. The two beams were repaired in flexion with one 6-mm-diameter NSM CFRP rod and then they were tested in three-points bending test up to failure. Overall stiffness and crack maps before and after repairing were studied. Ultimate capacity, ductility and failure mode are also discussed. The experimental results showed that the NSM technique increases the overall capacity (ultimate load capacity and stiffness) of control and corroded beams and allows restoring a sufficient ductility for repaired corroded elements and then restoring safety margin despite a non-classical mode of failure with the separation of concrete cover which happened in the corroded beam due to damage induced by corrosion. Finally some comparisons were made between experimental and FE numerical modeling results in order to study the specific mode of failure of corroded beam which happened by the separation of concrete cover.

INTRODUCTION

Corrosion of reinforcing steel is still a very important area of study for reinforced concrete structures as the cost increase due to the repairing of corroded RC structures worldwide exceeds $1.8 trillion per year (Schmitt, 2009). Many researches have been conducted in order to assess the damages of corroded RC structures. (Al-Sulaimani et al., 1990; Andrade et al., 1991; Cairns et al., 2005) presented those damages starting from reduction of cross sectional area of steel and reduction of its ductility ending with cracking and bonding problems in the RC elements which leads to the early failure of structures.

The near surface mounted reinforcement technique (NSM) is one of the promising techniques used nowadays for strengthening the deteriorated structures. In the NSM technique, the Carbon Fibre Reinforced Polymer (CFRP) rods are placed inside pre-cut grooves and are bonded to the concrete with epoxy adhesive, (De Lorenzis and Teng, 2007) showed some of the advantages of the NSM technique

over the conventional strengthening technique using externally bonded FRP laminates: (1) less consuming time during the installation process; (2) protected from natural and accidental damages and (3) the NSM technique has better bonding as the FRP rod in this case is fully embedded.

(Kreit et al., 2011) and (Al-Mahmoud et al., 2009) indicated that the use of NSM reinforcement can significantly improve the flexural performance of the RC beams throughout increasing the ultimate load-bearing capacity. The experimental data presented by (Al-Mahmoud et al., 2009) was used later by (Hawileh, 2012) who presented FEM model that can predict the ultimate capacity of RC beams subjected to 4-point loading using the commercial FEM software ANSYS, it was found that the diameter of FRP reinforcement rod has a crucial effect on the stiffness and the ultimate capacity of the RC beams strengthened with NSM, the use of 16 mm diameter FRP rod increased the ultimate capacity by 83.6% compared to that beam strengthened with 6 mm diameter rod.

The FEM program ABAQUS was used several times to simulate the RC beams as in (Lundqvist et al., 2005) that studied the anchorage length of CFRP rod in order to prevent the premature failure and (Radfar et al., 2012) who used ABAQUS to study the peeling-off failure mode in beams strengthened with externally bonded FRP laminates.

In this paper, an experimental and numerical modeling works of two reinforced concrete beams have been conducted. Mechanical and FEM experiments were performed on one strengthened corroded RC beam and one strengthened non-corroded beam in order to investigate the overall behavior, the ultimate load capacity and the failure mode of those beams.

EXPERIMENTAL PROGRAM

An experimental program was started at LMDC in 1984 aimed to understand the effects of the steel corrosion on the structural behavior of the RC elements. Many experimental studies were conducted on those beams to evaluate the development of corrosion cracking, to measure chloride content and to analyze the change of the mechanical behavior (Castel et al., 2000; Vidal et al., 2007). The natural aggressive environment system is presented in (Kreit et al., 2011).

The beams studied in this paper are one corroded beam (called A1CL3-R) and one control beam (called A1T-R). A1CL3-R beam was damaged by long-term natural corrosion under sustained loading in three-point flexure to M_{ser}=14 kN.m and it was repaired using a rod of CFRP 6 mm diameter using NSM technique. The control beam A1T-R was repaired using the same method as the one used to repair the corroded beam A1CL3-R. The layout of the reinforcement is shown in Figure 1. For these beams, M_{ser} represented the maximum loading value versus the durability in an aggressive environment (serviceability limit-state requirements in an aggressive environment).

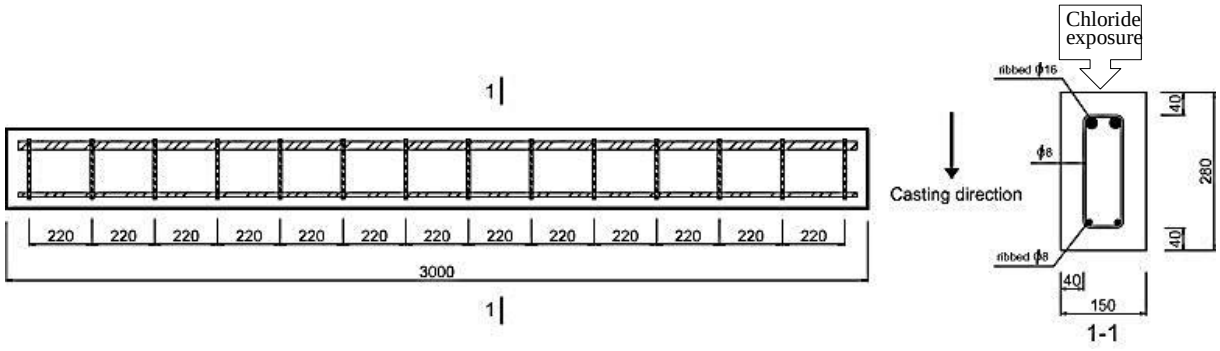

Fig. 1 Reinforcement Layout for Beams type A.

Material Properties

Concrete Properties

The average compression strength and the elastic modulus obtained on cylindrical specimens (ø11×22cm) were 45 MPa and 32 GPa respectively at 28 days. The tensile strength, measured using the splitting test, was 4.7 MPa. Porosity was 15.2%. To measure concrete characteristics nowadays, cylindrical cores 70 × 140 mm, were drilled out of each beam and were tested in both compression and tension. Table 1, gives the results of those core tests.

Table 1 Mechanical characteristics of the concrete.

Mechanical characteristics	A1CL3-R	A1T-R
Compression strength (MPa)	62.2	58.9
Tensile strength (MPa)	6.85	6
Elastic modulus (MPa)	34 000	30 000

Characterization of Steel Bars, CFRP Bars and Filling Material

The steel reinforcing bars were composed of natural S500 half-hard steels; ordinary ribbed reinforcing steel bars were used. The steel bars characteristics were measured after extracting the corroded steel bars out of the corroded beam A1CL3-R and non-corroded steel bar from control beam and they were found as in Table. 2. Table 3 shows the mechanical properties of the CFRP rods that found on that paper and the mechanical properties given by the manufacturer and by Laboratory test (AL-Mahmoud et al., 2007). In order to increase the bond between the CFRP rods and the filling material, the CFRP rods were coated with 0.2/0.3 mm of surface sanding material which was sprinkled onto an epoxy resin applied to the surface of the rods.

Table 2 Steel bars properties.

Specimen Type	Young's modulus (GPa)	Yield Strength (MPa)	Ultimate Strength (MPa)
Corroded specimen	200	578	710
Non-corroded specimen	214	600	645

Table 3 CFRP rods characteristics.

Type of test	Ultimate strength (MPa)	Modulus of Elasticity (MPa)
Manufacturer's test	2300	150000
Laboratory test[11]	1875	145900

Table 4, shows the characteristics of the filling material (epoxy resin) after 7 days (Kreit et al., 2011).

Table 4 Filling material properties.

Material	Compressive Strength (MPa)	Tensile Strength (MPa)	Elastic Modulus (MPa)
Epoxy	83	29.5	4900

NSM Repair Technique

The NSM CFRP rod was installed in the corroded beam A1CL3-R and in the control beam A1T-R by making two cuts in the concrete cover in the longitudinal direction at the tension side. A special concrete saw with a diamond blade was used. The groove was 15 mm deep (only 20 mm of concrete cover for beams) and 15 mm wide (around twice the rod diameter) (Al-Mahmoud et al., 2006). The two beams were tested after 1 week of installing the CFRP rod in order to ensure the maximum degree of adhesion between the concrete surface and the epoxy resin material. Figure 2 presents the main steps of this repairing process while figure 3 shows the final shape of the repaired beams after leveling their surfaces.

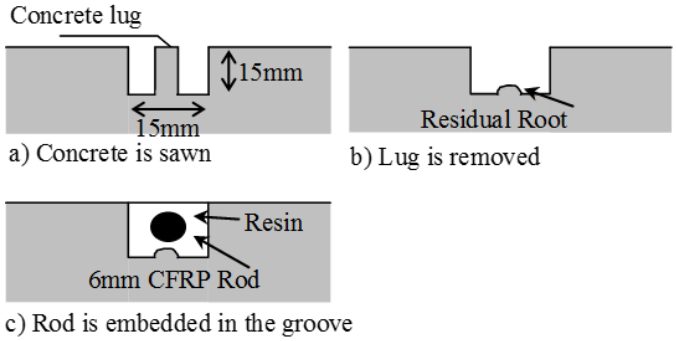

Fig. 2 Installation of CFRP rod into concrete surface.

a. A1T Control.Beam b. A1CL3 Corroded. Beam

Fig. 3. Concrete surface after installing the CFRP rod.

EXPERIMENTAL RESULTS

Corrosion Results for Steel Bars and Steel Stirrups for Corroded Beam A1CL3-R

The values of the diameter losses were measured for both the Back Side (BS) and Front Side (FS) tensile steel bars which were extracted from the corroded beam A1CL3-R just after the bending test. The maximum diameter loss was found 38% at 120 cm away of the left edge of the beam. The corrosion was found both at the top of the bars close to the surface cover reflected the classical result for natural corrosion (Yuan et al., 2007) and at the bottom of the bars reflected the effect of casting direction and bar location at the top of the beam known as "Top-bar effect" (Horne et al., 2007; Soylev and François, 2003). Figure 4 shows the diameter loss percentage along the corroded beam A1CL3-R for both tensile bars BS and FS.

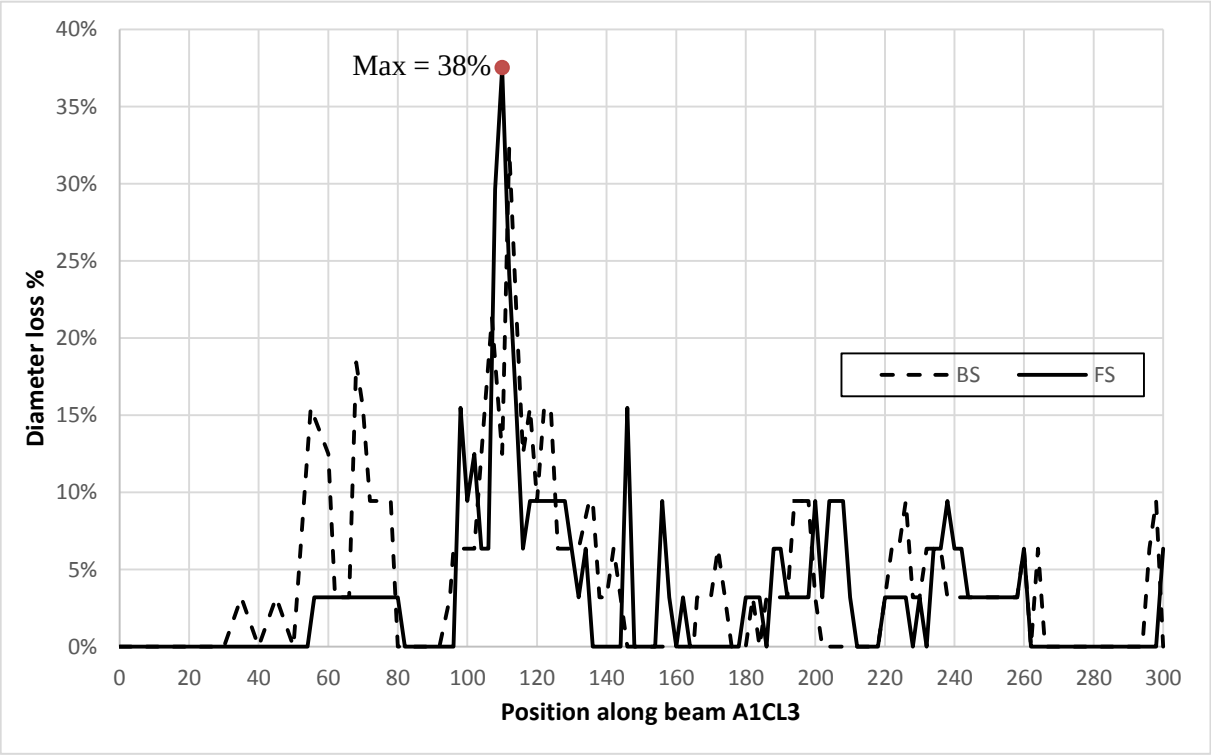

Fig. 4 Diameter loss percentage in corroded beam A1CL3-R.

The steel stirrups were numbered regarding to their parts (the first number represents the part's number and the second number represents the stirrup's number) as shown in Figure 5:

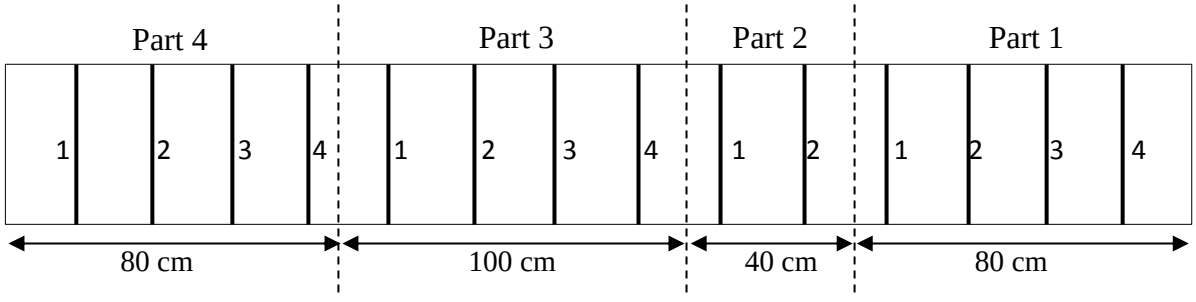

Fig. 5 Parts of beam A1CL3-R.

Figure 6 shows the locations of corrosion in the steel stirrups and the residual diameter values:

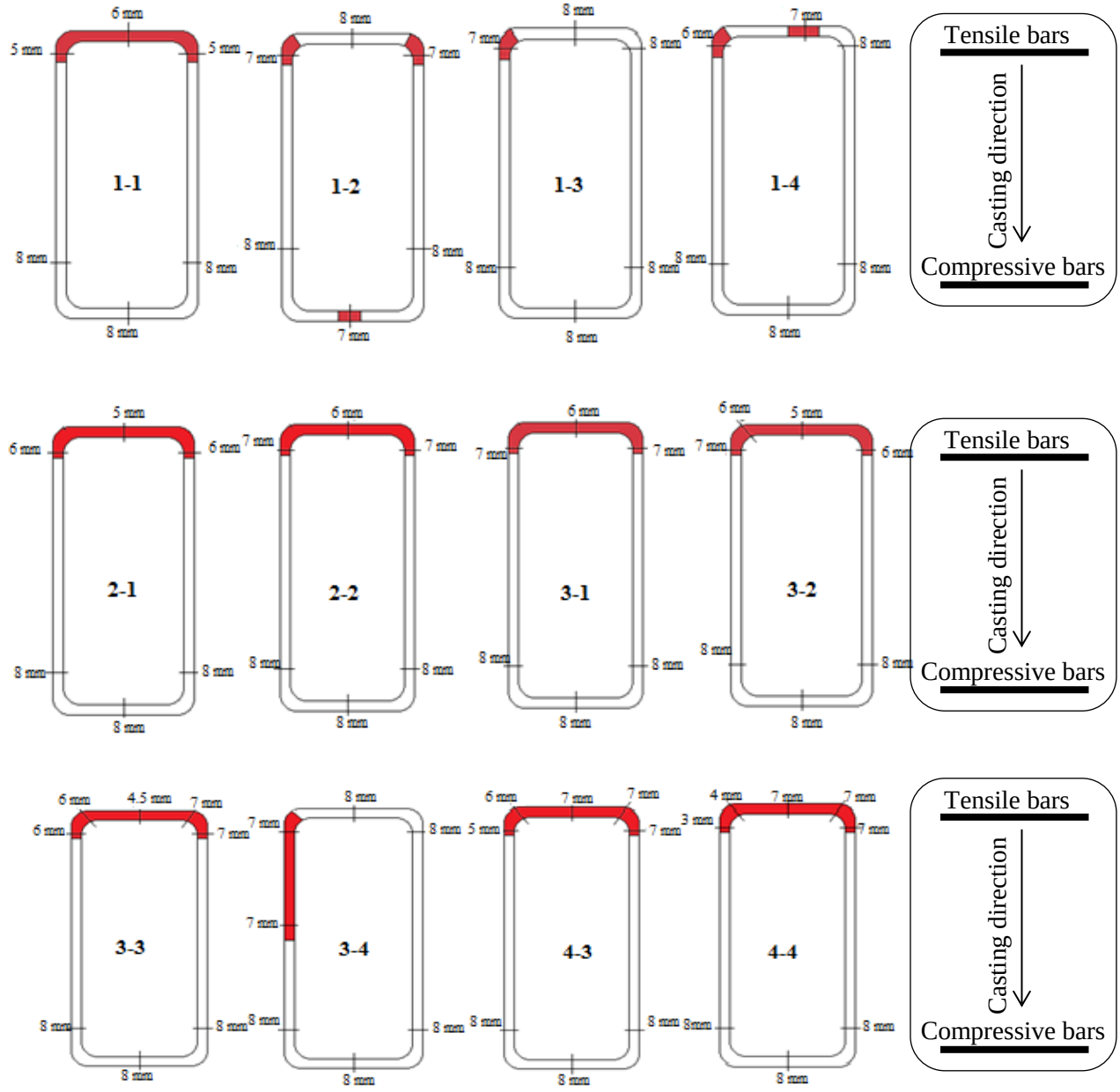

Fig. 6 Corrosion in steel bars of A1CL3-R

Stirrups corrosion is mostly located on the horizontal part of stirrups which are located at the top of the beam according to the casting direction which is related to the tensile steel bars corrosion while compressive steel bars reflect corrosion pits only.

Ultimate Load Capacity

The two repaired beams A1CL3-R and A1T-R were tested with 3-point loading up to failure. Figure 7 shows the bending moment versus the deflection for the two beams. The ultimate moment values were 52 kN.m and 66 kN.m respectively.

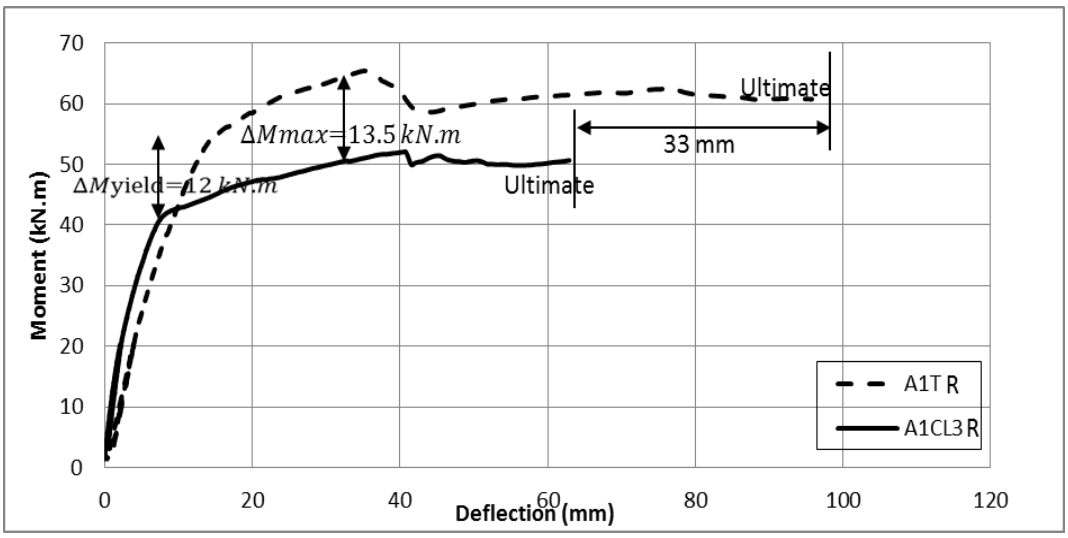

Fig. 7 Bending moment versus deflection

Increase Percentage in Yielding Moment Capacity for Repaired Beams with NSM

An increase in yielding moment happened due to NSM technique. An increase percentage of 19% (Table 5) was predicted in the repaired corroded beam A1CL3-R compared to the non-repaired one while this theoretical increase of 18% was experimentally verified for the repaired control beam A1T-R compared to a non-repaired control beam tested by (Khan et al., 2012) named A2T which had shown a yielding moment value of 44 kN.m.

Table 5. Increase percentage due to NSM.

Beam	My, repaired (kN.m) Recorded value.	My, non-repaired (kN.m) Calculated value	Increase percentage
A1CL3-R	43.5	36.5	19
A1T-R	51.7	43.7	18

NUMERICAL MODELING PROGRAM

The objective of this part is to create a reliable numerical model that can accurately predict the moment deflection curve, the global behavior and the mode of failure of corroded and control RC beams strengthened with NSM FRP rod. The numerical analysis consists of a three dimensional nonlinear finite element analysis using the commercial program ABAQUS.

Materials Models

The concrete and the filling material (Epoxy resin) are simulated using a 3-D deformable solid structural element in ABAQUS while the 3-D deformable wire is used to simulate the steel bars, the steel stirrups and the CFRP NSM rod reinforcement using a truss element. The steel loading plate and the steel supports are simulated using a 3-D deformable solid element and they are given higher yield values than the steel bars and stirrups in order to prevent the early yielding case.

Concrete

The mechanical behavior of concrete is difficult to simulate due to the complex behavior in traction and compression and the brittle cracking behavior of concrete, nowadays many models can simulate the concrete material in different approaches such as the concrete smeared cracking (Chaudhari and Chakrabarti, 2012; Si-Larbi et al., 2012), the concrete damaged plasticity (Abdullah and Mokhatar, 2012; Lundqvist et al., 2005) and the discrete cracking approach (Yang et al., 2003).

(1). Concrete in Compression

In this study, the mechanical properties of concrete found experimentally listed in Table 1 are used in ABAQUS in order to define the characteristics of concrete material with a Poisson's ratio of 0.2. The plastic behavior of concrete in compression is defined using the Drucker-Prager yield function which is controlled by the Drucker-Prager hardening variables in tension and compression. The Drucker-Prager criterion is a smooth approximation of Mohr-Coulomb yield surface and it is controlled with two parameters cohesion C and internal angle of friction ∅, it can be expressed using equation (1):

$$f(I_1, J_2) = \alpha I_1 + \sqrt{J_2} - k = 0 \qquad Eq.(1)$$

While: α, k are Drucker-Prager material constants, I_1 is the first invariant of the effective stress tensor and J_2 is the second invariant of the stress deviator tensor. In case that the Drucker-Prager is passing the inner cone of the tension meridian of the Mohr-Coulomb hexagon the Drucker-Prager constants will be expressed using equations (2):

$$\alpha = \frac{2\sin\emptyset}{\sqrt{3}(3+\sin\emptyset)}, k = \frac{6c\cos\emptyset}{\sqrt{3}(3+\sin\emptyset)} \qquad Eq.(2)$$

The two parameters cohesion C and internal angle of friction ∅ are assumed to be C =2.8 MPa and ∅ = 32˚ recommended by (Lubliner et al., 1989). The results of the experimental concrete specimens tested in compression are used in ABAQUS to fill in the Drucker-Prager hardening values while the same Young's modulus of concrete beams shown in Table.1 are used.

(2). Concrete in tension

The concrete tensile strength values of concrete are less than the compressive values and the concrete failure is brittle in tension, the same modulus of elasticity and Poisson's ratio are used here using the same tensile strength values obtained by the uniaxial traction tests shown in table 1.

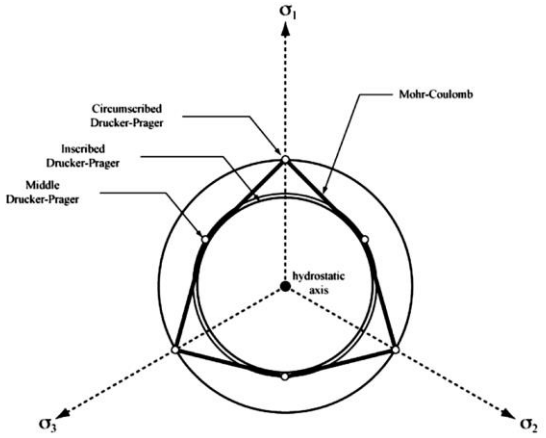

Fig. 9 Drucker-Prager failure criterion in stress space (Alejano and Bobet, 2012)

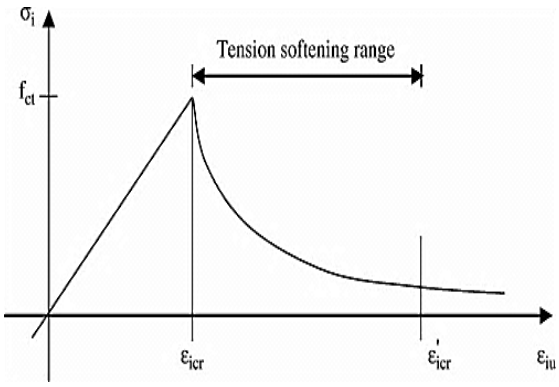

Fig. 10 Tension softening of concrete

Steel Bars and Stirrups

The nonlinear behavior of the steel reinforcement bars is considered to be linear elastic- plastic behavior. A Poisson's ratio of 0.3 is used while the elastic modulus and yield strength values of steel reinforcement bars and stirrups are used as in Table 2. The post yielding hardening behavior of steel bars is used as shown in figure 11.

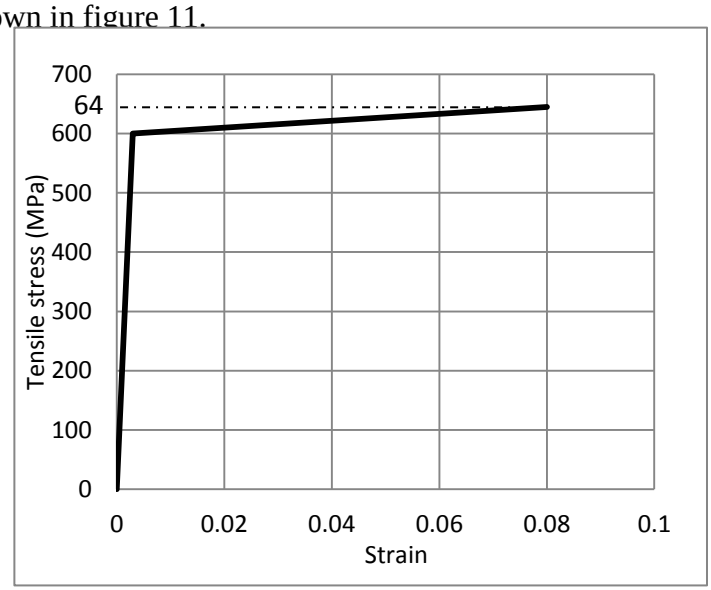

Fig. 11 Post yielding behavior of steel bars

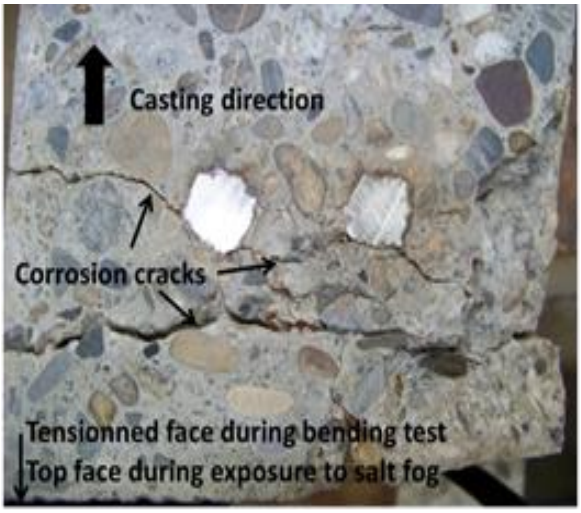

Fig. 12 Corrosion cracks appear in the concrete cover from the steel part closest to the tensioned surface exposed to chloride for A1CL3-R

The corrosion cracks shown in figure 12 are considered to be the main reason behind getting the separation of concrete cover as a mode of failure for the repaired corroded beam. This plane of cracks was simulated using a crack tool in interaction section in ABAQUS as shown in figure 13. As well as the cross-sectional area of tensile steel bars of corroded beam A1CL3-R are reduced due to the corrosion and they are given an average corrosion value (15% for tensile steel bars) at the middle of the beam as shown in corrosion percentage map in Figure 4.

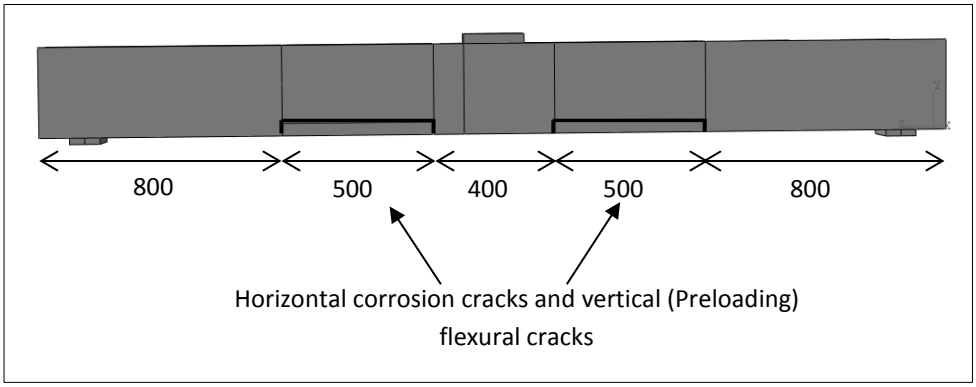

Fig. 13 Cracks created at concrete cover plane of corroded beam in (mm)

FRP Rods and Filling Material

The mechanical properties of the epoxy resin and FRP rod used here in this model are the same found by experimental tests table 3 and 4. The filling material is modeled as a 3-D solid element while the cracking model of concrete is used here as well in order to simulate the plastic behavior of epoxy material. The FRP rod is modeled with elastic stress-strain curve up to brittle failure in tension and zero strength in compression (Hawileh, 2012).

FEM Numerical Model

General

A 3-D finite element model is created using the commercial FE program ABAQUS which uses a non-linear static procedure with classical Full-Newton solving method. The beam could be entered as a full beam or the symmetry conditions can be used, in this study the full beam is modeled using suitable boundary conditions as shown in figure 14 with all the material discussed previously are inserted which are given the same mechanical properties taken from experimental tests.

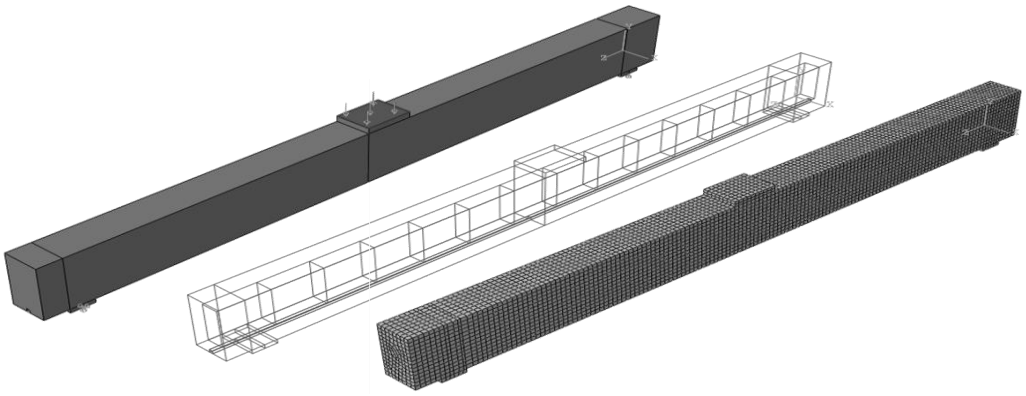

Fig. 14 Boundary conditions, steel skeleton and meshing of beam model

In this study as the main objective is to discuss the separation of concrete cover failure mode so the full bond is assumed between FRP and concrete as well as between steel skeleton and concrete material which was also assumed by (Radfar et al., 2012) to model a non-conventional failure mode (peeling-off).

Meshing and Step Size Increments

Four FEM models consisting of different meshing edge sizes of 20, 15, 10 and 5 mm in the concrete elements were compared in this paper in order to find out whether the meshing size has an effect on maximum failure load. In order to ensure the maximum degree of accuracy the maximum number of increments is entered as large values (100,000 increments) while the minimum increment size is entered as a small value (1E-08).

FEM Results

Ultimate Load Capacity

Three FEM models were created for repaired control beam (FEM A1T-R), repaired corroded beam without simulating the corrosion cracks (FEM A1CL3-R1) and repaired corroded beam with taking into account the corrosion cracks (FEM A1CL3-R2), mesh size value of 20 mm was used for the three models, the Moment-deflection curve for each beam was drawn at the mid-span point, figure 15 shows a good agreement between FEM moment-deflection curves for both beams compared to the experimental results.

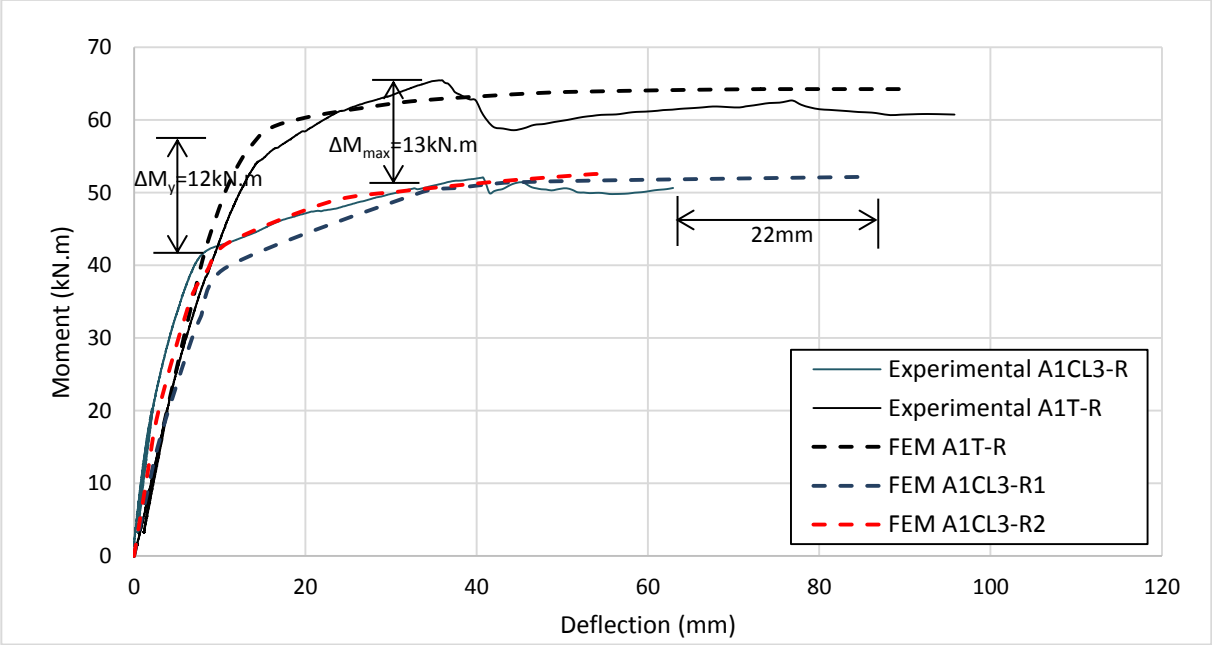

Fig. 15 Experimental Vs FEM results

The results show also that the corroded non-cracked beam FEM A1CL3-R1 has higher deflection values than the experimental corroded beam with 22 mm difference, while when the corrosion crack line was defined in order to simulate the premature failure it gave less deflection values than the non-cracked one and closer results to the experimental one. Table 6, presents a comparison between experimental and FEM results for each beam in terms of yielding moment, ultimate moment and ultimate deflection.

Table 6. FEM Vs Exp results

Beam	Yielding moment (kN.m)	Ultimate moment (kN.m)	Ultimate deflection (mm)
Experimental A1CL3-R	42.3	52	63
FEM A1CL3-R1	39.7	52.2	85
FEM A1CL3-R2	43	52.6	55
Experimental AT-R	53	65.5	93
FEM A1T-R	58.3	64.3	90

Mesh Size Effect on the Ultimate Capacity

Different mesh sizes are used in this part of analysis (20, 15, 10 and 5mm) in order to study the effect of changing elements sizes during the analysis, figure 16 shows that there was no significant effect on the ultimate moment value for control beam A1T-R and corroded beam A1CL3-R if the mesh size is changed which agrees with what is found by (Radfar et al., 2012).

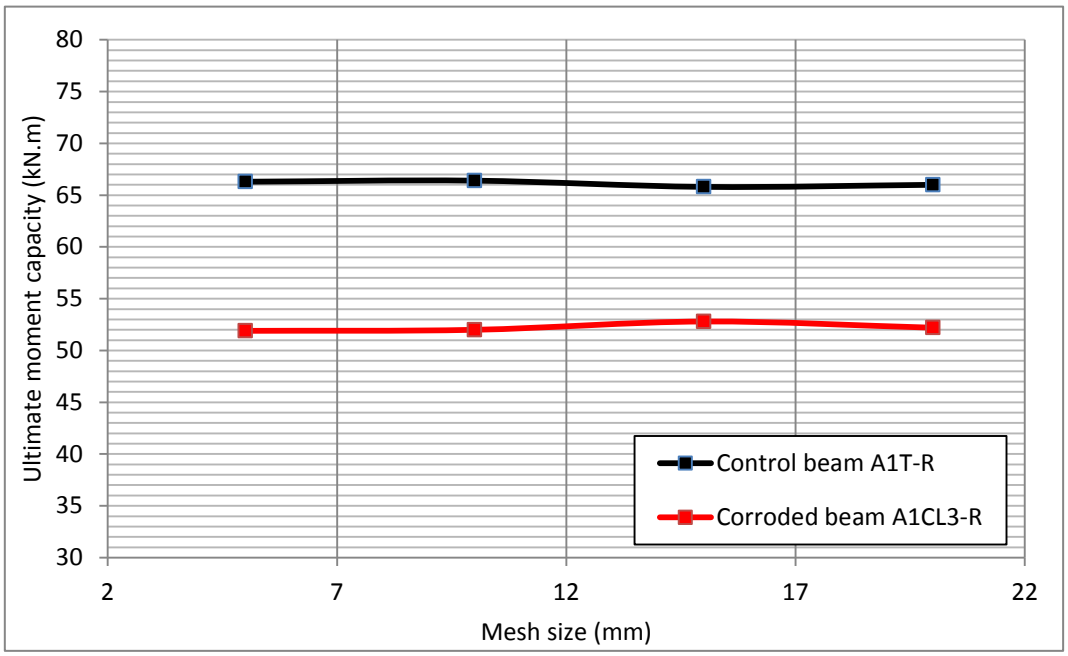

Fig. 16 Mesh size effect

Failure modes investigation

The failure mode of non-repaired type A beams usually happens due to steel bar yielding followed by concrete crushing (Khan et al., 2012). After strengthening with NSM FRP rod, the RC beams may fail by concrete crushing, pull-out of the FRP rods or peeling-off as shown by (Al-Mahmoud et al., 2009), the failure mode of the repaired control beam A1T-R occurred by the crushing of compressed concrete while the failure mode observed for A1CL3-R was different from both the conventional and non-conventional failure modes found on non-corroded repaired beams. The failure mode of the repaired corroded beam A1CL3-R was due to the separation of the concrete cover as shown in Figure 17.

a) A1CL3-R Corroded a) A1T-R Control Beam

Fig. 17 Experimental Failure modes of both beams

In order to define the crack lines along the concrete cover of the corroded RC beam FEM A1CL3-R2 several steps were conducted (ABAQUS/CAE User's Manual):

1. Several partitions were drawn just at the concrete cover place as shown in figure 13.
2. The crack line was defined using a crack tool from the interaction module in ABAQUS by selecting element edges of the partitioned parts which form continuous lines.
3. The crack extension direction was defined normal to the crack plane (across the beam width) in order to simulate the corrosion cracks described in figure 12.

4. Finally a seam crack was defined along the crack plane edges, this crack is defined by ABAQUS as an edge or a face in the model which is originally closed but can open during the analysis.

Moreover the existing vertical flexural cracks were added as shown in figure 13 in order to simulate the real state of the pre-loading process of the corroded beam. After ABAQUS finished the calculation process the concrete cover near the middle of the beam was separated as shown in figure 18.

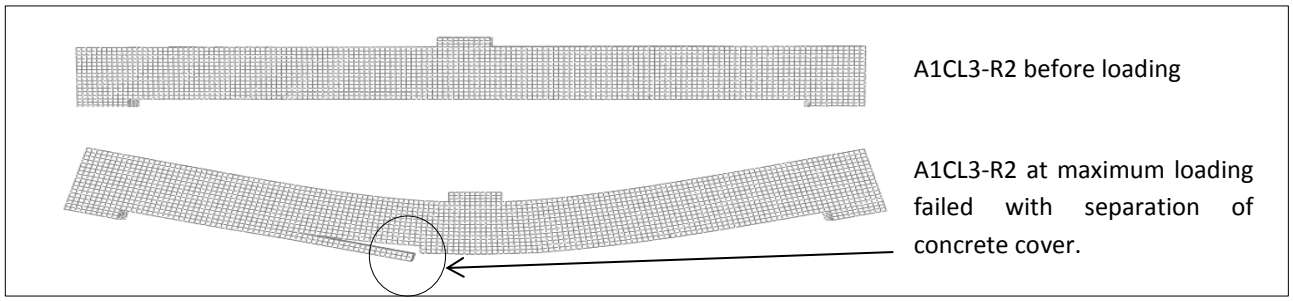

Fig. 18 Failure mode obtained for corroded beam A1CL3-R by FEM

CONCLUSIONS

According to the results found on this paper, the following conclusions could be listed:

1. The damage induced by corrosion modifies the flexural response of repaired corroded beam and lead to a new non-conventional failure mode by separation of concrete cover in the plane defined by corrosion cracks.
2. FEM analysis using ABAQUS is able to predict both load-bearing capacity and ultimate deflection reduction due to corrosion if crack plane induced by corrosion is taken into account in the model
3. NSM technique used to repaired corroded RC elements allow to restore a significant ductility by avoiding premature failure of tensile bars at pit location, nevertheless, the presence of cracks induced by corrosion coincident to the tensile reinforcement induced a new premature failure mode

REFERNCES

- Abdullah, R., Mokhatar, S.N., 2012. Computational analysis of reinforced concrete slabs subjected to impact loads. Int. J. Integr. Eng. 4, 70–76.
- Al-Mahmoud, F., Castel, A., François, R., Tourneur, C., 2009. Strengthening of RC members with near-surface mounted CFRP rods. Compos. Struct. 91, 138–147.
- Al-Mahmoud, F., Castel, A., François, R., Tourneur, C., Marchand, J., Bissonnette, B., Gagné, R., Jolin, M., Paradis, F., 2006. Anchorage and tension-stiffening effect between Near-Surface-Mounted Fiber Reinforced polymer rod and concrete. Presented at the Second international symposium on advances in concrete through science and engineering, Quebec-Canada.
- Al-Sulaimani, G., Kaleemullah, M., Basunbul, I., 1990. Rasheeduzzafar,(1990)"Influence of corrosion and cracking on bond behaviour and strength of reinforced concrete members" ACI Structural Journal, 87 (2), 220-231. ASTM G1.
- Alejano, L.R., Bobet, A., 2012. Drucker–Prager Criterion. Rock Mech. Rock Eng. 1–5.
- Al-Mahmoud Firas, Castel, A., François, R., Tourneur, C., 2007. Effect of surface pre-conditioning on bond of carbon fibre reinforced polymer rods to concrete. Cem. Concr. Compos. 29, 677–689.
- Andrade, C., Alonso, C., Garcia, D., Rodriguez, J., 1991. Remaining lifetime of reinforced concrete structures: Effect of corrosion on the mechanical properties of the steel.
- Cairns, J., Plizzari, G.A., Du, Y., Law, D.W., Franzoni, C., 2005. Mechanical properties of corrosion-damaged reinforcement. ACI Mater. J. 102.

- Castel, A., François, R., Arliguie, G., 2000. Mechanical behaviour of corroded reinforced concrete beams—Part 1: experimental study of corroded beams. Mater. Struct. 33, 539–544.
- Chaudhari, S., Chakrabarti, M., 2012. Modeling of concrete for nonlinear analysis Using Finite Element Code ABAQUS. Int. J. Comput. Appl. 44.
- De Lorenzis, L., Teng, J., 2007. Near-surface mounted FRP reinforcement: An emerging technique for strengthening structures. Compos. Part B Eng. 38, 119–143.
- Hawileh, R.A., 2012. Nonlinear finite element modeling of RC beams strengthened with NSM FRP rods. Constr. Build. Mater. 27, 461–471.
- Horne, A., Richardson, I., Brydson, R., 2007. Quantitative analysis of the microstructure of interfaces in steel reinforced concrete. Cem. Concr. Res. 37, 1613–1623.
- Khan, I., François, R., Castel, A., 2012. Structural performance of a 26-year-old corroded reinforced concrete beam. Eur. J. Environ. Civ. Eng. 16, 440–449.
- Kreit, A., Al-Mahmoud, F., Castel, A., François, R., 2011. Repairing corroded RC beam with near-surface mounted CFRP rods. Mater. Struct. 44, 1205–1217.
- Lubliner, J., Oliver, J., Oller, S., Oñate, E., 1989. A plastic-damage model for concrete. Int. J. Solids Struct. 25, 299–326.
- Lundqvist, J., Nordin, H., Täljsten, B., Olofsson, T., 2005. Numerical analysis of concrete beams strengthened with CFRP-A study of anchorage lengths. Presented at the Proceedings, International Symposium on Bond Behaviour of FRP in Structures (BBFS 2005), Hong Kong, China, pp. 247–254.
- Radfar, S., Foret, G., Saeedi, N., Sab, K., 2012. Simulation of concrete cover separation failure in FRP plated RC beams. Constr. Build. Mater. 37, 791–800.
- Schmitt, G., 2009. Global needs for knowledge dissemination, research, and development in materials deterioration and corrosion control. World Corros. Organ. N. Y.
- Si-Larbi, A., Agbossou, A., Ferrier, E., Michel, L., 2012. Strengthening RC beams with composite fiber cement plate reinforced by prestressed FRP rods: Experimental and numerical analysis. Compos. Struct. 94, 830–838.
- Soylev, T., François, R., 2003. Quality of steel–concrete interface and corrosion of reinforcing steel. Cem. Concr. Res. 33, 1407–1415.
- Vidal, T., Castel, A., François, R., 2007. Corrosion process and structural performance of a 17 year old reinforced concrete beam stored in chloride environment. Cem. Concr. Res. 37, 1551–1561.
- Yang, Z., Chen, J., Proverbs, D., 2003. Finite element modelling of concrete cover separation failure in FRP plated RC beams. Constr. Build. Mater. 17, 3–13.
- Yuan, Y., Ji, Y., Shah, S.P., 2007. Comparison of two accelerated corrosion techniques for concrete structures. ACI Struct. J. 104.